Article:

Liu, Y. orcid.org/0000-0003-3034-9628, Jin, X. orcid.org/0000-0002-7205-3318, Jung, H. orcid.org/0000-0002-5250-4767 et al. (5 more authors) (2024) Electroabsorption in InGaAs and GaAsSb p-i-n photodiodes. Applied Physics Letters, 125 (22). 221107. ISSN 0003-6951

https://doi.org/10.1063/5.0228938

Applied Physics Letters

RESEARCH ARTICLE | NOVEMBER 26 2024

Electroabsorption in InGaAs and GaAsSb *p-i-n* photodiodes

Y. Liu ; X. Jin ; H. Jung ; S. Lee ; F. Harun ; J. S. Ng ; S. Krishna ; J. P. R. David

Appl. Phys. Lett. 125, 221107 (2024)
https://doi.org/10.1063/5.0228938

Applied Physics Letters ARTICLE pubs.aip.org/aip/apl

Electroabsorption in InGaAs and GaAsSb *p-i-n* photodiodes

Cite as: Appl. Phys. Lett. **125**, 221107 (2024); doi: 10.1063/5.0228938
Submitted: 16 July 2024 · Accepted: 16 November 2024 · Published Online: 26 November 2024

Y. Liu,[1] X. Jin,[1,a)] H. Jung,[2,3] S. Lee,[2,3] F. Harun,[4] J. S. Ng,[1] S. Krishna,[2] and J. P. R. David[1]

AFFILIATIONS

[1]Department of Electronic and Electrical Engineering, University of Sheffield, Sheffield S1 3JD, United Kingdom
[2]Department of Electrical and Computer Engineering, The Ohio State University, Columbus, Ohio 43210, USA
[3]Department of Electrical Engineering, University of Texas at Arlington, Arlington, Texas 76019, USA
[4]Electronics Technology Section, Universiti Kuala Lumpur British Malaysian Institute, Gombak, Selangor Darul Ehsan 53100, Malaysia

[a)]Author to whom correspondence should be addressed: xjin4@outlook.com

ABSTRACT

The application of an electric field to a semiconductor can alter its absorption properties. This electroabsorption effect can have a significant impact on the quantum efficiency of detector structures. The photocurrents in bulk InGaAs and GaAsSb *p-i-n* photodiodes with intrinsic absorber layer thicknesses ranging from 1 to 4.8 μm have been investigated. By using phase-sensitive photocurrent measurements as a function of wavelength, the absorption coefficients as low as 1 cm^{-1} were extracted for electric fields up to 200 kV/cm. Our findings show that while the absorption coefficients reduce between 1500 and 1650 nm for both materials when subject to an increasing electric field, an absorption coefficient of 100 cm^{-1} can be obtained at a wavelength of 2 μm, well beyond the bandgap energy when they are subject to a high electric field. The results are shown to be in good agreement with theoretical models that use Airy functions to solve the absorption coefficients in a uniform electric field.

Accurate knowledge of the optical absorption coefficient is crucial for designing optoelectronic devices, such as photodetectors (PDs), avalanche photodiodes (APDs), and modulators. $In_{0.53}Ga_{0.47}As$ and $GaAs_{0.5}Sb_{0.5}$, both with direct bandgaps of approximately 0.75 eV and capable of being grown lattice matched to InP, are utilized as absorber materials for 1550 nm telecommunications applications, and understanding their absorption characteristics is important. The absorption in $In_{0.53}Ga_{0.47}As$ (hereafter InGaAs) has been previously studied, with transmission measurements performed on epitaxially grown samples demonstrating absorption coefficients from 30 000 to 20 cm^{-1} across wavelengths from 1000 to 1700 nm, respectively.[1] These findings agreed well with earlier studies by Humphreys *et al.*[2] and Zielinski *et al.*[3] Hahn *et al.*[4] extended this research by using transmission and reflectance spectroscopy to study how the electron doping concentration affects intrinsic absorption in InGaAs, observing a notable shift in the fundamental absorption edge toward shorter wavelengths due to the band-filling effect. Work on the absorption coefficients in $GaAs_{0.5}Sb_{0.5}$ (hereafter GaAsSb) also lattice matched to InP is more scarce with initial work by Park and Jang,[5] based on transmission measurements on a 1 μm MOVPE grown GaAsSb/InP heterostructure layer. More recently, Lee *et al.*[6] reported on the absorption properties of two MBE grown GaAsSb samples, where there was good agreement with Park and Jang[5] except at the longer wavelengths near the band edge.

The growing demand for increased network bandwidth and capacity has resulted in the expansion of operational wavelengths in optical fibers from C-band (1530–1565 nm) to L-band (1565–1625 nm), which has the second lowest attenuation.[7] These wavelengths lie close to the band edges of the InGaAs and GaAsSb absorber materials where the absorption coefficients can be significantly influenced by external electric fields—an important consideration when using them in photodiodes, APDs, and other optoelectronic devices such as optical modulators and switches. The electroabsorption effect, described independently by Franz[8] and Keldysh,[9] introduces an electric-field-dependent absorption "tail" in bulk semiconductors through photon-assisted tunneling of electrons from valence to conduction bands.

In this work, by utilizing thick epitaxially grown absorption layers of InGaAs and GaAsSb in a *p+-i-n+* configuration and measuring their wavelength dependent photocurrents, absorption coefficients as low as 1 cm^{-1} have been obtained over the wavelength range of 1200–1830 nm in the absence of any externally applied field. By applying a reverse bias voltage to the devices, changes to the absorption just above and below the band edge in InGaAs and GaAsSb are investigated for electric fields up to 200 kV/cm, and the electroabsorption coefficient has been experimentally determined for wavelengths up to 2200 nm. Good agreement is found between the measurements and calculated absorption coefficients using the theoretical model of Tharmalingam[10] and Callaway.[11]

Two *p-i-n* structure photodiodes of InGaAs and two of GaAsSb were grown using Metalorganic vapor-phase epitaxy (MOVPE) and Molecular Beam Epitaxy (MBE), respectively. They were both fabricated into circular mesa diodes using standard photolithography and wet chemical etching, with the diameters of the diodes ranging from 100 to 500 μm.

Each of these structures features highly doped ($>10^{18}\,\mathrm{cm}^{-1}$) $p+$ and $n+$ cladding layers at the top and bottom, respectively, as shown in Fig. 1(a). These are wide-bandgap materials of InP for the InGaAs structures and InAlAs for the GaAsSb structures to ensure that no light is absorbed over the wavelength range of interest. Each structure also has a thin 20 nm highly $p+$ doped InGaAs contacting layer. The two InGaAs *p-i-ns* had 4.8 and 1.8 μm thick intrinsic layers (referred to as InGaAs A and InGaAs B, respectively), while the GaAsSb *p-i-ns* had intrinsic regions of 1.8 and 1.0 μm (referred to as GaAsSb A and GaAsSb B, respectively). To confirm the background doping and intrinsic layer widths, capacitance–voltage (CV) measurements were undertaken, as shown in Fig. 1(b). For all the layers, the capacitance scales with area and reduces rapidly within 1 V, indicating that the background doping level in the intrinsic region is low. The low background doping in all these structures means that the electric field (and therefore the absorption coefficient) can be assumed to be constant across the depletion region, simplifying the experimental analysis. The forward dark currents for the four samples had ideality factors that range from 1.3 to 1.7.

For an accurate determination of the absorption coefficient, the wavelength dependence of the photocurrent in the devices was measured using a grating monochromator and a tungsten halogen light source. A phase sensitive lock-in technique was used to eliminate any contribution due to dark currents and background noise to the measurements. The external quantum efficiencies at 0 V were calculated by comparing the photocurrents with a calibrated extended InGaAs photodiode[12] and are shown in Fig. 2(a). This extended InGaAs photodiode was also used to correct for the system response for all the photocurrent and external quantum efficiencies shown in this work.

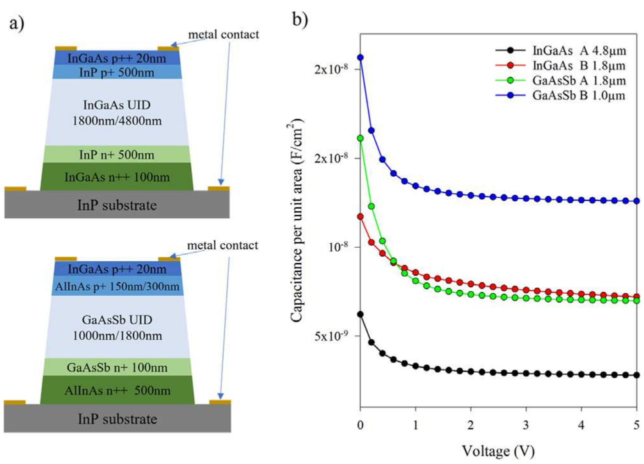

FIG. 1. (a) Cross-sectional schematics of InGaAs and GaAsSb heterojunction photodiodes. (b) Capacitance–voltage data for InGaAs (black and red) and GaAsSb (green and blue).

For all the structures, the cladding layers can be considered transparent for wavelengths beyond 1 μm. Any light absorbed in the very thin doped contact layers is assumed to only slightly reduce the calculated quantum efficiency by $\sim$1% and is ignored. Therefore, the external quantum efficiency (EQE) generated from the intrinsic region is given by

$$EQE\,(\lambda) = (1 - R)e^{-\alpha(\lambda)t_p}[1 - e^{-\alpha(\lambda)t_i}], \tag{1}$$

where R is the reflection loss of the top surface, $\alpha(\lambda)$ is the wavelength dependent absorption coefficient, t_p is the width of the top contact layer ($\sim$20 nm), and t_i is the width of intrinsic layer. The reflection at the air-semiconductor interface is calculated using the reflectivity data obtained by Bacher,[1] while the reflectivity between the *i*-region and the cladding layers is neglected due to their similar refractive indices.

The extracted 0 V absorption coefficients for InGaAs and GaAsSb from 1400 nm are shown in Fig. 2(b). These coefficients are almost identical (within experimental errors) for diodes with different intrinsic (*i*-region) widths. Uncertainties in our measurements are small due to the phase sensitive techniques enabling small values of photocurrent to be measured accurately. Systematic errors arising from small uncertainties in absorption layer thickness ($\pm 0.05\,\mu$m from CV measurements) lead to an error of $\pm$1% in extracted absorption coefficients. The results also agree well with the published absorption coefficients for InGaAs[1,2,4] and GaAsSb[5] but are shown here with absorption determined down to 1 cm^{-1}. The absorption coefficients for GaAsSb and InGaAs are 8400 and 8100 cm^{-1} at 1550 nm, respectively. Figure 2(b) shows that at zero bias, the absorption coefficient decreases almost exponentially with increasing wavelengths beyond the bandgap, and the rate of decrease is similar in both materials and for different thicknesses. This broadening of the absorption edge can be quantified by Urbach's rule[13] as

$$E_u = \left[\frac{d[\ln(\alpha)]}{d(\hbar\omega)}\right]^{-1}, \tag{2}$$

where E_u is the Urbach energy, α is the absorption tail below the bandgap, and $\hbar\omega$ is the energy of photon. This long wavelength broadening is believed to originate from optically induced electronic transitions due to multiple phonon absorptions in crystalline materials,[14] internal electric fields caused by impurities, and by alloy disorder.[15] E_u for both InGaAs and GaAsSb was found to be 7.68 meV for InGaAs A, 7.92 meV for InGaAs B, 8.69 meV for GaAsSb A, and 8.53 meV for GaAsSb Hanh *et al.*[4] obtained a larger value of 13 meV for E_u in InGaAs, but this was for *n*-doped layers.

Having established the zero bias absorption coefficients, we next explore how they evolve when the photodiodes are subjected to increasing external electric fields. Figures 3(a) and 3(b) present the measured EQE spectra at various reverse biases in the 4.8 μm InGaAs and 1 μm GaAsSb devices, respectively. Initially, the EQE shows a broadening of the absorption edge to longer wavelengths at low voltages, but then the entire EQE starts to increase rapidly at bias voltages

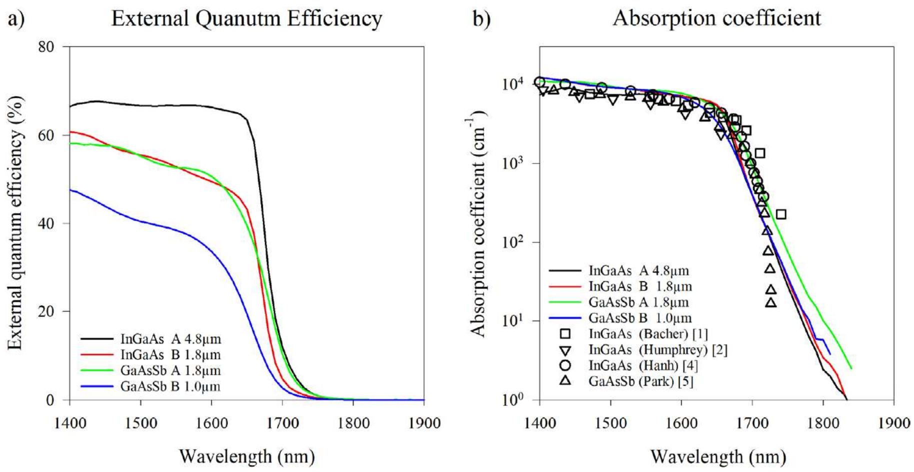

FIG. 2. The (a) external quantum efficiency and (b) absorption coefficient of the InGaAs and GaAsSb photodiodes with different *i*-region thicknesses at 0 V bias.

beyond 40 V in Fig. 3(a) and beyond 16 V in Fig. 3(b). The other two InGaAs and GaAsSb devices showed very similar behavior. Reversed biased photodiodes can undergo avalanche multiplication even under moderate electric fields, especially in the case of InGaAs.[16] This amplified changes in the EQE at high biases must be corrected for when determining the electric field dependence of the absorption coefficients. The avalanche multiplication in the 4.8 μm InGaAs and 1 μm GaAsSb devices is calculated as a function of reverse bias using their respective impact ionization coefficients with[16,17]

$$M_x = \frac{\exp\left[-\int_0^x \left(\alpha_{ic}(x') - \beta_{ic}(x')\right)dx'\right]}{1 - \int_0^w \alpha_{ic}(x')\exp\left[-\int_0^{x'} \left(\alpha_{ic}(x'') - \beta_{ic}(\beta_{ic}'')\right)dx''\right]dx'}, \quad (3)$$

where M_x is the multiplication due to the initiating carrier being generated at position x, W is the width of the high field depletion region, α_{ic} is the electron impact ionization coefficient, and β_{ic} is the hole impact ionization coefficient.

At short wavelengths, in these *p-i-n* structures, electrons initiate the avalanche multiplication process (M_e), and at longer wavelengths, where the photons are absorbed in the high field region, both electrons and hole initiate the multiplication process. The red curves in Fig. 3(c) are the multiplication characteristics arising from a uniform generation of electron and holes in the absorption region, i.e., when the absorption coefficient is very small, defined as M_{mix}. As α_{ic} is larger than β_{ic} (especially at low electric fields in the InGaAs[16]), M_e is larger than M_{mix}, as shown in Fig. 3(c). At the longer wavelengths being investigated here, this M_{mix} is more likely to be responsible for the multiplication we observe, so by dividing the EQE shown in Figs. 3(a) and 3(b) by their respective M_{mix} curves, the unmultiplied EQE could be determined. In reality, the value of M_{mix} will be larger than that shown by the red lines at shorter wavelengths as electron-initiated ionization becomes more important, but this only adds a small error of $<$10% to the value of the unmultiplied EQE over the wavelength range of interest.

The electric field dependent absorption coefficients that are deduced from the unmultiplied EQE spectra are shown by the symbols in Fig. 4. For both InGaAs and GaAsSb, the absorption coefficients increase with electric field at wavelengths beyond 1660 nm in InGaAs

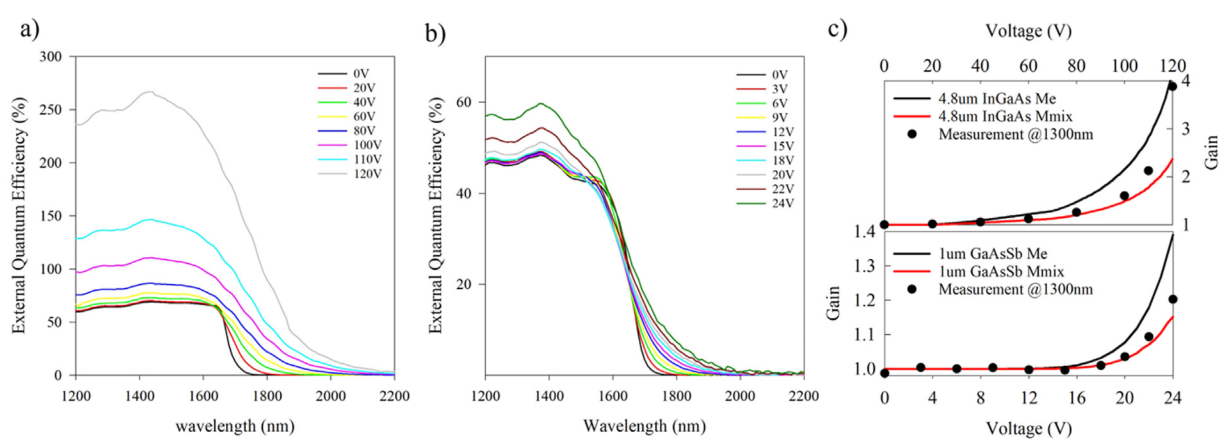

FIG. 3. The external quantum efficiency spectrum of (a) 4.8 μm InGaAs A and (b) 1 μm GaAsSb B under various reverse bias. (c) Calculated multiplication factors (Me and Mmix) and measured gain at 1300 nm as a function of reverse bias voltage for the same devices.

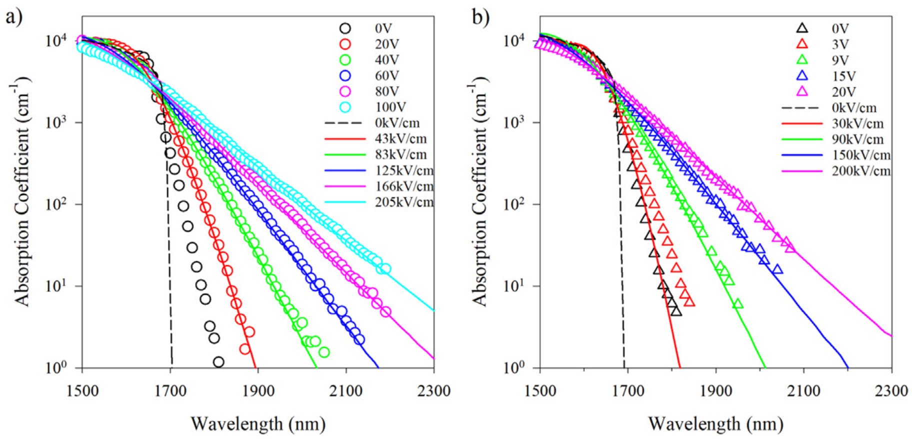

FIG. 4. The extracted and calculated absorption coefficients under various reverse bias for (a) InGaAs and (b) GaAsSb photodiodes.

and 1650 nm in GaAsSb, leading to a softening of the roll-off slopes and a red-shift of the cutoff edge. The energy where these electroabsorption curves intersect each other (i.e., are almost independent of electric field) is sometimes referred to as the "neutral point,"[18] and this gives values for InGaAs (0.747 eV) and GaAsSb (0.751 eV) that are in close agreement with literature values for E_g. At the highest electric fields investigated of 200 kV/cm, the absorption coefficients at 2000 nm have increased from effectively zero to 96 cm^{-1} for InGaAs and 66 cm^{-1} for GaAsSb, indicating their potential for high contrast waveguide modulation at this wavelength.

To understand the effect of the electric-field on the absorption coefficients, we have attempted to model the electroabsorption due to the Franz-Keldysh effect. The Franz-Keldysh effect, described by Franz[8] and Keldysh[9] in the late 1950s, involves the tilting of the conduction and valence bands due to an electric field, leading to quantum mechanical tunneling of electrons from the valence band to the conduction band. Tharmalingam[10] and Callaway[11] introduced an effective mass approximation and used an Airy function for the numerical calculation of the oscillations and decay with photon energy of the electroabsorption coefficient.

The equations to determine the electroabsorption coefficients as given by Tharmalingam[10] and Callaway[11] are

$$\alpha(\hbar\omega, F) = A \times F^{\frac{1}{3}}\left[\left|\frac{d\,Ai(\beta)}{d\,\beta}\right|^2 - \beta\left|Ai(\beta)\right|^2\right], \tag{4}$$

where

$$\beta = B \times \left(E_g - \hbar\omega\right)F^{-2/3}, \tag{5}$$

where $Ai(\beta)$ is the Airy function, F is the electric field, $\hbar\omega$ is the energy of the photons, and E_g is the bandgap energy. A is given by Alping[19] as

$$A = \frac{C}{n\hbar\omega}\left(\frac{2\mu}{m_0}\right)^{4/3}, \tag{6}$$

while B is given by both Stillman[20] and Alping[19] as

$$B = 1.1 \times 10^5 \left(\frac{2\mu}{m_0}\right)^{1/3}, \tag{7}$$

where m_0 is the free electron mass, μ is the reduced mass defined by $\mu = \frac{m_e^* m_h^*}{m_e^* + m_h^*}$, where m_e^* and m_h^* are the relative electron and hole masses, respectively, and n is the refractive index. The pre-factor C in Eq. (6), which is associated with the inter-band matrix elements, is a tunable parameter to be aligned with the empirical zero-field absorption coefficient data.[21,22]

The value of E_g that has to be used in Eq. (5) to fit to the measured data is ∼12–17 meV smaller than the conventionally accepted values and is referred to as the effective bandgap E_{ge} in Table I. The few publications that compare calculated and measured electroabsorption coefficients show poor agreement, and it is unclear that what value of E_g was used in their models. Leeson *et al.*[22] also had to use E_g values for GaAs that were smaller than the normally accepted 1.42 eV value in his analysis and to fit the data of Wight *et al.*[18] Bhowmick *et al.*[23] recently suggested that fitting to a materials absorption coefficient gives a value of E_g that is smaller, and so we feel that these effective E_{ge} values should be used to calculate the electroabsorption coefficients. The only other parameters that are adjustable are the constant C in Eq. (6) and the reduced mass, μ. These parameters alongside the refractive index n are shown in Table I. The calculated electroabsorption coefficients as a function of wavelength using these parameters are represented by the lines in Fig. 4. These lines agree closely with the experimental data at the higher electric fields. Similarly, good agreement between calculations and measurements was obtained for InGaAs B and GaAsSb A (not shown) when the same constants are used in Eqs. (4)–(7). As a result, the electroabsorption coefficients can be calculated for any device with a InGaAs or GaAsSb absorption region using these parameters. At low electric fields, the agreement between the model and measurements is less good as the Urbach broadening sets the lowest practicable measured roll-off.

TABLE I. The parameters for the calculated absorption coefficient of InGaAs and GaAsSb. Also included is the neutral point for the electroabsorption coefficients.

	InGaAs	GaAsSb
Refractive index, n	3.56	3.65
C	7.2×10^4	6.5×10^4
Effective reduced mass, μ	0.0278	0.0330
Effective bandgap, E_{ge}	0.733 eV (1690 nm)	0.738 eV (1680 nm)
Neutral point, E_g	0.747 eV (1660 nm)	0.751 eV (1650 nm)

TABLE II. Summary of mass parameters used for InGaAs and GaAsSb.

	InGaAs	GaAsSb
Electron mass, m_e	0.041	0.0447
Light hole mass, m_{lh}	0.052	0.066
Heavy hole mass, m_{hh}	0.363	0.455
Light-hole electron reduced mass, μ_{lh}	0.0227	0.0267
Heavy-hole electron reduced mass, μ_{hh}	0.0368	0.0407

It can be seen from Eqs. (4)–(7) that the calculation of electroabsorption coefficients relies on not only the zero-field absorption (as an arbitrary fitting parameter) but also the reduced effective mass μ. More importantly, μ determines the rate of change of the electroabsorption coefficients with the electric field, and Kingston[24] has suggested that this will be similar for all semiconductors with a similar value of μ. From published values of the electron, light-hole, and heavy-hole masses in InGaAs[25] and GaAsSb,[26] we get values of μ_{lh} and μ_{hh} for each material, as shown in Table II. Several authors[18,22,27] have used a single effective reduced mass in their calculations of the electroabsorption coefficients for GaAs, and we replicated their simulation results by applying their published reduced mass values to Eqs. (4)–(7). For our measurements, we find that using a single value ($\mu = 0.0278$ for InGaAs and $\mu = 0.0330$ for GaAsSb) between μ_{lh} and μ_{hh} as given in Table II gives the best fit. Leeson and Payne[22] calculated the electroabsorption coefficient of InGaAs using a larger value of $\mu = 0.038$. While using this value of μ with the equations presented in this work gives similar electroabsorption coefficients to Leeson and Payne,[22] the absolute values do not agree with the experimental results shown in Fig. 4(a) or the calculations with $\mu = 0.0278$.

A comparison of the electroabsorption between InGaAs and GaAsSb using the parameters in Table II shows that there is a slightly larger change with electric field for the InGaAs due to its smaller reduced mass. It is not possible to calculate the electroabsorption coefficients from first principles due to the large number of unknown parameters, but using this physics-based model with a few adjustable parameters enables us to empirically fit to experimental results and can help with the device design.

Figure 5(a) shows how the absorption coefficients decrease with increasing electric field at wavelengths of 1550 and 1600 nm. At 1600 nm, the absorption coefficients decrease from 7113 to 5225 cm^{-1} in InGaAs and from 7101 to 5710 cm^{-1} in GaAsSb as the electric field increases from zero to 150 kV/cm. For a 1 μm thick absorber region, this change at 1600 nm will lead to a notable decline in the internal quantum efficiency (IQE), dropping from 50.8% to 40.7% for InGaAs, and from 50.8% to 43.45% for GaAsSb. This decrease is less pronounced at 1550 nm. In reality, both the electroabsorption reduction and avalanche multiplication may be happening simultaneously to the photons absorbed in the absorber region at high electric fields, making the overall effect less obvious (especially in InGaAs).

Figure 5(b) also shows that wavelengths beyond the optical bandgap can be detected with increasing efficiency as the electric field increases. These properties could be exploited in waveguide devices to extend the wavelength of conventional short wavelength infrared detectors and APDs albeit at the expense of higher dark currents due to tunneling. These results suggest that photocurrent spectral measurements in APD structures, such as those with separate absorption, charge, and multiplication (SACM) configurations, can provide critical information on the electric field distribution within the InGaAs or GaAsSb absorber regions. This insight is valuable for optimizing device design, especially considering the performance constraints introduced by the variations in absorption coefficients in SACM structures, even under relatively low electric fields, which are typical operating conditions for many InGaAs SACMs.[28,29]

In conclusion, we have conducted experimental measurements and theoretical modeling of the electroabsorption coefficients in bulk

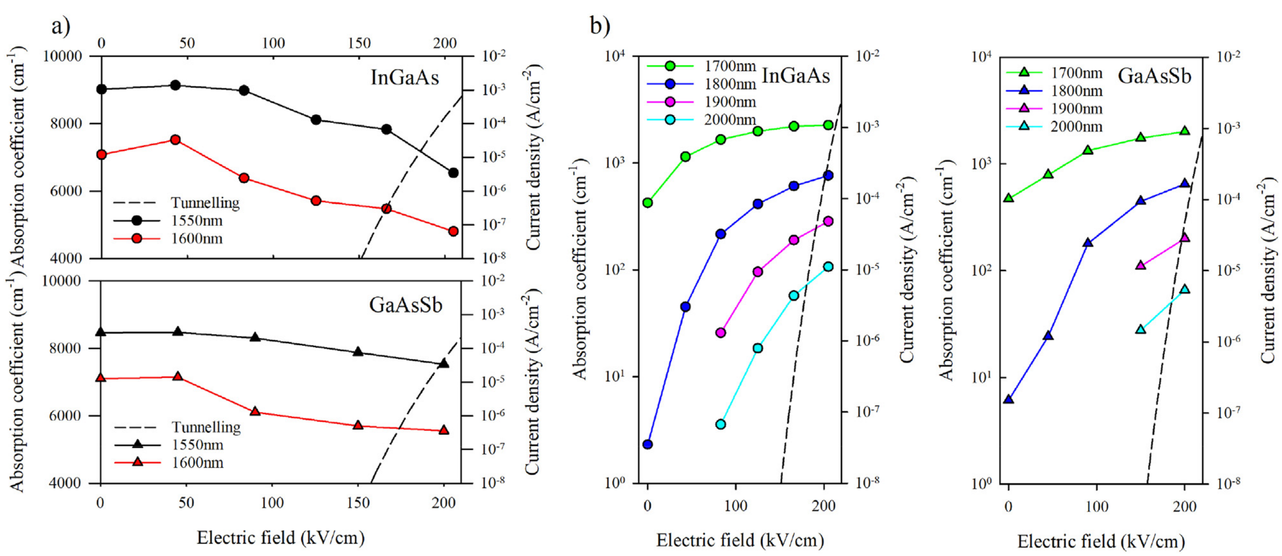

FIG. 5. The electroabsorption coefficients as a function of electric field for InGaAs (circles) and GaAsSb (triangles) at (a) 1550 nm (black), 1600 nm (red), also shown is the tunneling dark current density for these two materials as a function of the electric field. (b) Increasing absorption coefficient with an electric field at 1700 nm (green), 1800 nm (blue), 1900 nm (purple), and 2000 nm (cyan).

InGaAs and GaAsSb under electric fields up to ~200 kV/cm. These measurements reveal significant changes in the absorption properties both above and below the bandgap energies of these materials. Theoretical modeling of the electroabsorption effect has shown excellent agreement with the experimental results, validating the accuracy of the model.

This work was partially supported by the Advanced Component Technology (ACT) Program of NASA's Earth Science Technology Office (ESTO) (Grant No. 80NSSC21K0613).

AUTHOR DECLARATIONS

Conflict of Interest

The authors have no conflicts to disclose.

Author Contributions

Y. Liu: Conceptualization (lead); Data curation (lead); Formal analysis (lead); Investigation (lead); Validation (lead); Visualization (lead); Writing – original draft (lead); Writing – review & editing (lead). **X. Jin:** Conceptualization (lead); Data curation (lead); Formal analysis (lead); Investigation (lead); Validation (lead); Visualization (lead); Writing – original draft (equal); Writing – review & editing (equal). **H. Jung:** Data curation (equal); Formal analysis (equal); Investigation (equal); Validation (equal); Writing – review & editing (equal). **S. Lee:** Data curation (equal); Formal analysis (equal); Investigation (equal); Validation (equal); Writing – review & editing (equal). **F. Harun:** Conceptualization (equal); Data curation (equal); Formal analysis (equal); Investigation (equal); Validation (equal); Writing – review & editing (equal). **J. S. Ng:** Conceptualization (equal); Data curation (equal); Formal analysis (equal); Investigation (equal); Supervision (supporting); Visualization (equal); Writing – review & editing (equal). **S. Krishna:** Conceptualization (equal); Data curation (equal); Formal analysis (equal); Funding acquisition (equal); Investigation (equal); Supervision (equal); Validation (equal); Writing – review & editing (equal). **J. P. R. David:** Conceptualization (equal); Data curation (equal); Formal analysis (equal); Funding acquisition (equal); Investigation (equal); Methodology (equal); Supervision (equal); Validation (equal); Writing – original draft (equal); Writing – review & editing (equal).

DATA AVAILABILITY

The data that support the findings of this study are available from the corresponding author upon reasonable request.

REFERENCES

[1]F. R. Bacher, J. S. Blakemore, J. T. Ebner, and J. R. Arthur, "Optical-absorption coefficient of In1−xGaxAs/InP," Phys. Rev. B **37**(5), 2551–2557 (1988).

[2]D. A. Humphreys, R. J. King, D. Jenkins, and A. J. Moseley, "Measurement of absorption coefficients of Ga0.47In0.53As over the wavelength range 1.0–1.7 μm," Electron. Lett. **21**(25–26), 1187 (1985).

[3]E. Zielinski, H. Schweizer, K. Streubel, H. Eisele, and G. Weimann, "Excitonic transitions and exciton damping processes in InGaAs/InP," J. Appl. Phys. **59**(6), 2196–2204 (1986).

[4]D. Hahn, O. Jaschinski, H.-H. Wehmann, A. Schlachetzki, and M. Von Ortenberg, "Electron-concentration dependence of absorption and refraction in n-In0.53Ga0.47As near the band-edge," J. Electron. Mater. **24**(10), 1357–1361 (1995).

[5]M. S. Park and J. H. Jang, "GaAs0.5Sb0.5 lattice matched to InP for 1.55 um photo-detection," Electron. Lett. **44**(8), 549 (2008).

[6]S. Lee, X. Jin, H. Jung, H. Lewis, Y. Liu, B. Guo, S. H. Kodati, M. Schwartz, C. Grein, T. J. Ronningen, J. P. R. David, J. Campbell, and S. Krishna, "High gain, low noise 1550 nm GaAsSb/AlGaAsSb avalanche photodiodes," Optica **10**(2), 147 (2023).

[7]L. Rapp and M. Eiselt, "Optical amplifiers for multi–band optical transmission systems," J. Lightwave Technol. **40**(6), 1579–1589 (2022).

[8]W. Franz, "Einfluß eines elektrischen Feldes auf eine optische Absorptionskante," Z. Für Naturforsch. A **13**(6), 484–489 (1958).

[9]L. V. Keldysh, "Ionization in the field of a strong electromagnetic wave," in *Selected Papers of Leonid V Keldysh* (World Scientific, 2023), pp. 56–63.

[10]K. Tharmalingam, "Optical absorption in the presence of a uniform field," Phys. Rev. **130**(6), 2204–2206 (1963).

[11]J. Callaway, "Optical absorption in an electric field," Phys. Rev. **130**(2), 549–553 (1963).

[12]Thorlabs, see https://www.thorlabs.com/thorcat/TTN/TTN035395-S01.pdf for "FD05D photodiode specifications (TTN035395-S01, Rev D)" (2017).

[13]M. V. Kurik, "Urbach rule," Phys. Status Solidi (a) **8**(1), 9–45 (1971).

[14]C. H. Grein and S. John, "Temperature dependence of the Urbach optical absorption edge: A theory of multiple phonon absorption and emission sidebands," Phys. Rev. B **39**(2), 1140–1151 (1989).

[15]B. Bansal, V. K. Dixit, V. Venkataraman, and H. L. Bhat, "Alloying induced degradation of the absorption edge of InAsxSb1−x," Appl. Phys. Lett. **90**(10), 101905 (2007).

[16]J. S. Ng, C. H. Tan, J. P. R. David, G. Hill, and G. J. Rees, "Field dependence of impact ionization coefficients in In0.53Ga0.47As," IEEE Trans. Electron Devices **50**(4), 901–905 (2003).

[17]H. Jung, S. Lee, Y. Liu, X. Jin, J. P. R. David, and S. Krishna, "High electric field characteristics of GaAsSb photodiodes on InP substrates," Appl. Phys. Lett. **122**(22), 221102 (2023).

[18]D. R. Wight, A. M. Keir, G. J. Pryce, J. C. H. Birbeck, J. M. Heaton, R. J. Norcross, and P. J. Wright, "Limits of electro-absorption in high purity GaAs, and the optimisation of waveguide devices," IEE Proc. J. Optoelectron. **135**(1), 39 (1988).

[19]A. Alping and L. A. Coldren, "Electrorefraction in GaAs and InGaAsP and its application to phase modulators," J. Appl. Phys. **61**(7), 2430–2433 (1987).

[20]G. E. Stillman, C. M. Wolfe, C. O. Bozler, and J. A. Rossi, "Electroabsorption in GaAs and its application to waveguide detectors and modulators," Appl. Phys. Lett. **28**(9), 544–546 (1976).

[21]B. R. Bennett and R. A. Soref, "Analysis of Franz-Keldysh electro-optic modulation in InP, GaAs, GaSb, InAs, and InSb," Proc. SPIE **836**, 158–168 (1987).

[22]M. S. Leeson and F. P. Payne, "Predicted performance of Franz-Keldysh effect optical reflection modulators and comparisons with similar multiple quantum well-based devices," IEE Proc. - Optoelectron. **141**(4), 257–264 (1994).

[23]M. Bhowmick, H. Xi, and B. Ullrich, "Absorption limit in direct gap III–V semiconductors," J. Appl. Phys. **134**(1), 015702 (2023).

[24]R. H. Kingston, "Electroabsorption in GaInAsP," Appl. Phys. Lett. **34**(11), 744–746 (1979).

[25]T. P. Pearsall, *GaInAsP Alloy Semiconductors* (Wiley, Chichester, West Sussex, 1982).

[26]M. Levinshtein, S. L. Rumyantsev, M. Shur, and W. Scientific, *Handbook Series on Semiconductor Parameters: Ternary and Quaternary III-V Compounds* (World Scientific Publishing Company, 1999).

[27]B. O. Seraphin and N. Bottka, "Franz-Keldysh effect of the refractive index in semiconductors," Phys. Rev. **139**(2A), A560–A565 (1965).

[28]G. S. Kinsey, J. C. Campbell, and A. G. Dentai, "Waveguide avalanche photodiode operating at 1.55 μm with a gain-bandwidth product of 320 GHz," IEEE Photonics Technol. Lett. **13**(8), 842–844 (2001).

[29]N. Duan, S. Wang, X. G. Zheng, X. Li, N. Li, J. C. Campbell, C. Wang, and L. A. Coldren, "Detrimental effect of impact ionization in the absorption region on the frequency response and excess noise performance of InGaAs-InAlAs SACM avalanche photodiodes," IEEE J. Quantum Electron. **41**(4), 568–572 (2005).